12th World Congress on Structural and Multidisciplinary Optimization
5th - 9th, June 2017, Braunschweig, Germany

Temperature Constraint Formulations for Heat Conduction Topology Optimization

Danny J. Lohan, James T. Allison

University of Illinois at Urbana-Champaign, Urbana, USA, {dlohan2, jtalliso}@illinois.edu

1. Abstract

In this paper an investigation of formulations for temperature constrained topology optimization is presented. This investigation is motivated by power electronics applications where the temperature requirements of several devices constrain the design of passive heat spreaders. Efficiently obtaining an accurate measure of temperature for use in density-based topology optimization is challenging. Enforcing point-wise distributed constraints increases the computational burden of the optimization, and utilizing global constraints often result in inaccurate constraint evaluations. Three maximum approximation functions are investigated as a means to improve the accuracy of the constraint evaluation. The soft maximum function is found to outperform the p-norm and is used in demonstrative examples. The accuracy of the soft maximum function is tested with both global and regional constraint implementations.

2. Keywords: Heat Conduction, Temperature Constraints, Density Methods, Max Approximations

3. Introduction

As power density continues to increase in today's electronics, efficient cooling becomes more challenging. Materials such as Gallium Nitride (GaN) have allowed for a decrease in switching device size, and as a result, a decrease in the system package size. The efficiency of conventional planar cooling strategies becomes limited with a new decrease in surface area. As an alternative, interleaved cooling presents a promising alternative where devices may be cooled from multiple sides. This paper presents the first steps in developing a topology optimization methodology for interleaved cooling. Designing an intricate cooling structure to increase power density requires accurate evaluations of temperature. In this paper, temperature-constrained topology optimization formulations are investigated for use in problems where heat conduction is the primary means of heat transfer.

There are many examples of topology optimization used in the design of heat spreading structures; refer to Dbouk (2017) for a recent review. A typical heat spreader topology optimization problem would minimize either thermal compliance, or temperature. However, temperature constraints can be utilized to allow for the use of a system level objective (Lohan et al, 2016). Topology optimization methods have matured for component-level design, however, lack in performance when the scope of design is increased. In this paper, an investigation is conducted to remedy issues with temperature-constrained topology optimization problems. Distributed temperature constraint formulations, such as those posed by Zhuang and Xiong (2015), consider point temperature constraints. In their paper, temperature was constrained on a few discrete several points on the domain. This assumption can not be made in compact power electronic applications where the heat sink size does not dwarf the circuit components. Solving this problem with a large number of point-wise constraints would require an increase in computational expense that makes problem solution impractical. In the domain of heat transfer, there has not been a thorough study of how to best manage temperature constraints in topology optimization. For relevant insight, the domain of structural mechanics can be examined.

An analogy can be drawn between temperature-constrained optimization problems in heat transfer and stress-constrained structural optimization problems. Both of these constraints need to be satisfied across the entire domain, and enforcing them in a point-wise manner results in an often intractable topology optimization problem. Researchers in structural mechanics have devised several methods for obtaining optimized solutions with reasonable computational efficiency; these have been compared in París et al (2010). The first of these strategies is the use of global constraint measures for optimization. For example, using a p-norm as a differentiable approximate maximum function (Duysinx and Sigmund, 1998). Another strategy is to enforce localized or regional constraints (Holmberg et al, 2013), where the global measure can be enforced in a specific region to improve accuracy. In a power electronics applications this is a useful method since the heat sensitive areas are defined a priori by the circuit layout and device characteristics. Further improvements in accuracy can be obtained by using an adaptively normalized constraint function (Le et al, 2010). The concepts described here will be implemented in this work to improve temperature-constrained topology optimization.

In this article, an investigation of temperature constraint formulations is presented. As power electronic systems have often have a large number of components, alternative global maximum approximations are considered. The following section describes the topology optimization methodology used herein. This is followed by an isolated investigation of 3 different maximum approximation functions. The findings are incorporated into an example temperature-constrained topology optimization problem to demonstrate feasibility.

4. Topology optimization methodology

The topology optimization can be posed in the following form:

$$\begin{aligned} \min_{\mathbf{d}} \quad & \Theta_0(\mathbf{d}) \\ s.t. \quad & \Theta_i(\mathbf{d}) < 0 \quad \forall i, \end{aligned} \tag{1}$$

where some objective Θ_0 is minimized with respect to the set of design variables, $\mathbf{d}$, subject to a set of constraints, Θ_i, where the subscript, i, is an index that differentiates the constraint number. The design variable, d, takes values between 0 and 1 to represent void and solid material properties. To solve this topology optimization problem, a density-based approach is used. The SIMP penalization scheme is used to penalize material with partial density:

$$\rho(d) = \alpha(d)\rho_0 = d^P \rho_0. \tag{2}$$

The material density, ρ, is scaled by a penalization function, α. In this study, a power function is used to scale the material properties, where the design variable, d, is raised to a power, P. The penalization parameter, P, is increased at intervals to produce a closer to binary design representation. A density filter is used to enforce a minimum radius constraint:

$$\rho(d_i) = \frac{\sum_{j\in\Omega_i} w_j \alpha(d_j)}{\sum_{j\in\Omega_i} w_j}, \qquad \text{where } w_j = \frac{r_{\min} - r_j}{r_{\min}}. \tag{3}$$

For an element , d_i, the filter has a domain, Ω_i, for which a weighting parameter, w_j, scales the density. The scaling parameters, w_j, are the ratio of the difference between the minimum radius, $r_{\min}$, and the distance between the two elements, r_j. The discrete adjoint method is used to obtain the sensitivities for optimization, and the globally convergent method of moving asymptotes is used to optimize the heat spreader design. To remedy some numerical instabilities, all the gradients are normalized, where the maximum gradient for each function is scaled to 1. The optimizer is set to converge by either a change smaller than 0.001 of the design variable, or a maximum of 100 iterations.

5. Maximum approximation functions

To reduce the computational expense of a temperature-constrained topology optimization problem, global measures to approximate the maximum function are investigated. Three different global measures of the maximum functions are chosen here. The first approximation function is used is the p-norm. This function approximates the max function as $p \to \infty$. It is given by the following equation:

$$x_{\text{norm}} = ||\mathbf{x}||_p = \left(\sum_{i=1}^{n} |x_i|^p \right)^{1/p}, \text{ where } \mathbf{x} \in \mathbb{R}^n. \tag{4}$$

This approximation has been used regularly for stress-constrained topology optimization. The next approximation function is the the smooth maximum function:

$$x_{\text{smooth}} = \frac{\sum_{i=1}^{n} x_i \exp(\alpha x_i)}{\sum_{i=1}^{n} (\exp(\alpha x_i))}, \tag{5}$$

where a scalar, α, is chosen to make the exponential finite. The final maximum approximation is the soft maximum function:

$$x_{\text{soft}} = \frac{1}{N} \ln \left(\sum_{i=1}^{n} \exp(N x_i) \right), \tag{6}$$

where the scalar, N, is also chosen to make the exponential finite. The three differentiable functions are compared using the following test problem:

$$x_{\max} = \max(x_1 = 1, x_2), \tag{7}$$

where the approximate function must determine the maximum number between the first number, x_1 (fixed at $x_1 = 1$), and the second number, x_2, which is varied. Continuous representations for the performance of the three approximate maximums are presented in Fig. 1

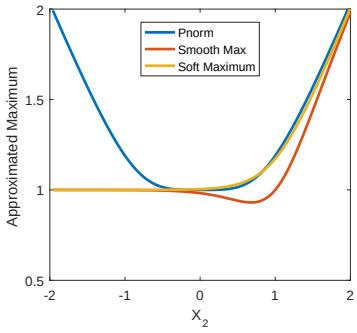

Figure 1: Maximum approximation functions.

To obtain this plot, the following values were chosen: $p = 10, \alpha = 1, N = 10$. From the figure, it is clear that each of these approximation functions is unique in its predictive capability. Furthermore, each of these functions has unique behaviors that restrict the modifications that can be made to increase the accuracy of the approximation. The p-norm function approximates the maximum absolute value of a set of numbers. This allows for free scaling, but restricted shifting of the number set when required. The smooth maximum function performs well for $|x_1 - x_2| \gg 0$, meaning the data set can be freely shifted, but must be carefully scaled. This approximate function works best when there is a large variation in the number set. The soft maximum approximation seems the most robust, where the correct approximation is made regardless of sign or variance in numbers. This test case provides some intuition on the performance of the functions, however, scaling is an important concern for all three function where inputting large values will result in undefined maximum approximations.

To obtain a better understanding of each function several additional tests are conducted. First, the scalar parameters in each approximation function are varied, illustrated in Fig. 2.

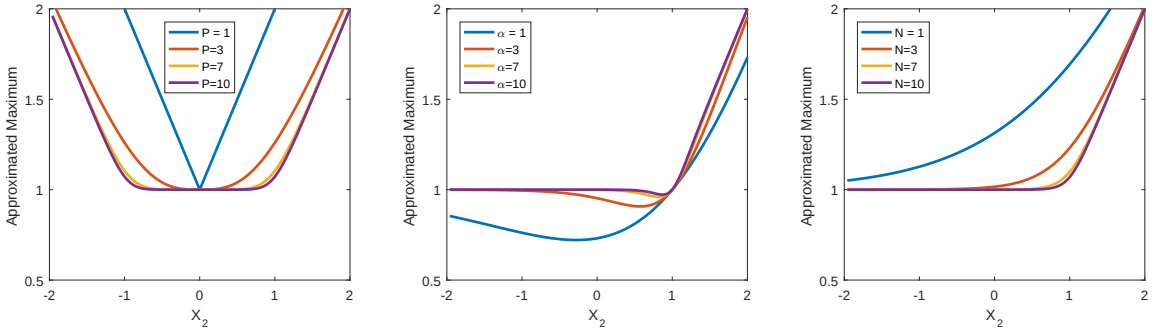

(a) Norm approximation (b) Smooth approximation (c) Soft approximation

Figure 2: Approximation scaling issues.

It is clear that there are further restrictions on the use of each function. The p-norm function losses differentiability as $p \to 1$ and $p \to \infty$, the smoothest gradient is obtained for an intermediate value of p. The smooth approximate max function loses accuracy quickly as $\alpha \to 1$. Furthermore, the derivative switches sign. This change in derivative sign is also present when x_1 and x_2 are nearly the same. The soft function also loses accuracy as $N \to 1$, however, the function is monotonically increasing. The shows initial promise in being a general use tool, compared to this other functions, which are restricted by number values.

5.1. Mesh depedency

The simple two number test presented in the last section provided some insight regarding the performance of each function. It was noted that the performance of each function depends somewhat on the difference between the two numbers being tested. To obtain a better sense of the performance of each function, these approximations will be tested as objective functions in topology optimization. This is done to isolate the approximation from the effects of an alternative objective function when used as a temperature constraints. Consider a solid copper plane (1 m $\times$ 1 m), with a volumetric heat generation of 1 W/m^2. The design domain (Fig. 3) is dominated by heat conduction and governed by Eqn. (8).

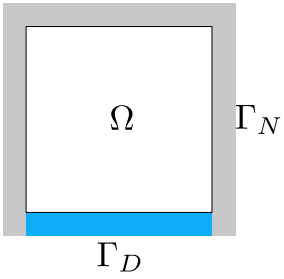

Figure 3: Test case domain.

$$\begin{aligned} \nabla(\kappa \nabla T) + g &= 0 \text{ on } \Omega \\ T &= 0 \text{ on } \Gamma_D \\ q &= 0 \text{ on } \Gamma_N \end{aligned} \tag{8}$$

The bottom edge of the plane has a fixed temperature constraint of 0° C, and the remaining edges are adiabatic.

The first test conducted is to gauge the performance of the approximate functions as mesh resolution increases. In this numerical experiment, the maximum temperature is approximated for a full copper plane. The mesh resolution is increased from 40 $\times$ 40 elements to 140 $\times$ 140 elements. To evaluate all of the functions fairly, the temperature used for the approximation is the normalized temperature on the domain.

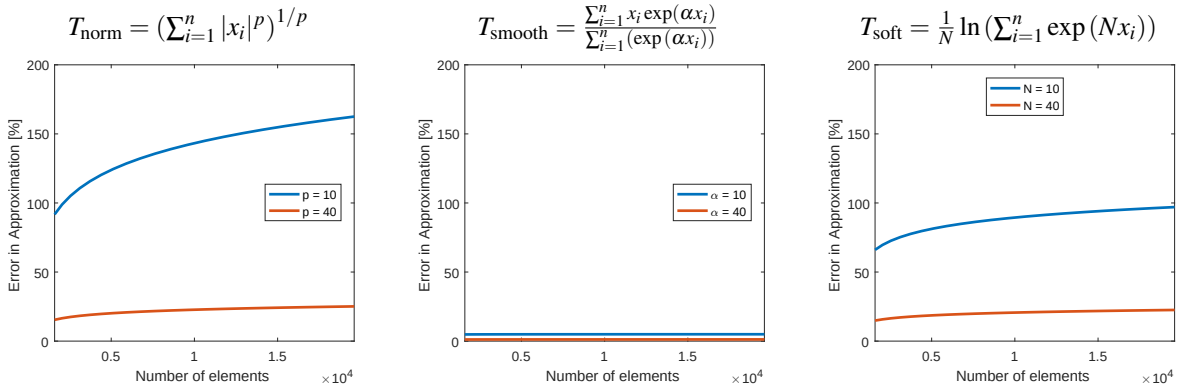

Figure 4: Accuracy as a function of mesh size.

The relative error for each approximate function is presented for two scalar levels at the various mesh sizes in Fig. 4. The same axis has been used for each approximation function to facilitate visual analysis. It can be seen that the smooth max function has the best predictive power for a given mesh size. The norm function has the worst scaling, and the soft maximum function is in between the two in performance. When using a global approximate function as a constraint, the relative error should be considered when deciding what safety factor to scale the constraint by.

5.2. Error Trajectory

The second experiment is to observe the accuracy of each norm function during optimization. It was noted that the accuracy of the approximate functions depend somewhat on the temperature distribution across the domain.

For this study, the domain is discretized into 160,000 elements and a minimum filter radius of 0.1 m is used. As the material properties are shifted on the domain, a larger variation on the spatial temperature variation is usually observed. The topology optimization will be carried out for 50 iterations, and the percentage error is plotted at each iteration.

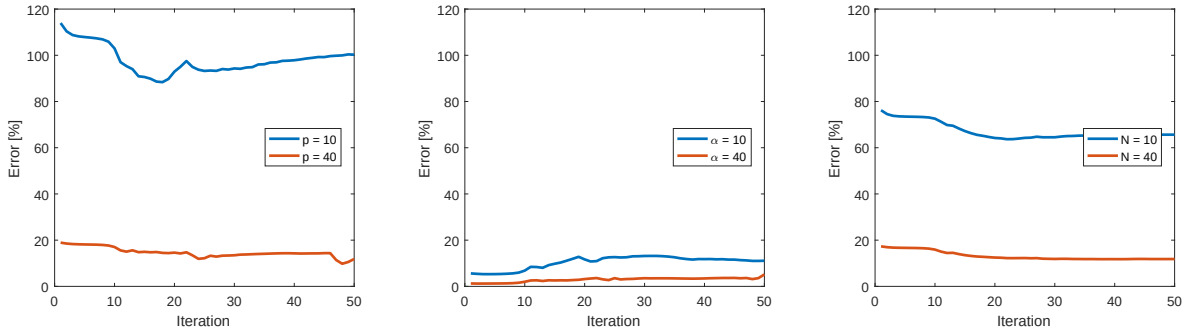

Figure 5: Error Trajectory through optimization iterations.

It is clear in all three graphs that increasing the scaling parameter causes large jumps in the accuracy of the approximate functions. Furthermore, during a single optimization, the error in maximum temperature may vary by 30 percent for the p-norm, 10 percent for the smooth max, and 20 percent for the soft max function. The variation seen here gives some insight that the gradients calculated will scale somewhat at each iteration. It cannot be assumed that when using a single scaling value, that the solution obtained at the final iteration will solve the same problem as posed in the first iteration.

5.3. Penalization Dependence

Final topologies can be analyzed to investigate penalization dependence. The final topologies obtained for each approximation function at various scaling parameters are given in Fig. 6. The p-norm function obtains different topologies for every different exponent value. Furthermore, as the norm penalty value increases, large oscillations in material distribution are observed during the optimization. Similar behavior can be seen when using the smooth maximum approximation, where a different topology is obtained for each different α parameter. The soft function, however, obtains the same topology for three different values of N. This is promising for topology optimization, where the design independence of optimization parameters is desirable.

6. Numerical examples

The following sections will present three examples where the softmax function is used to enforce temperature constraints.

6.1 Continuum Example

Consider the same homogeneously heated 1 m $\times$ 1 m design domain as described in the test cases. A compliance minimization problem is solved that satisfies the following problem formulation:

$$\begin{aligned} \min_{\mathbf{d}} \quad & \Theta_0(\mathbf{d}) = UP \\ s.t. \quad & \Theta_1(\mathbf{d}) = T(\mathbf{d}) \leq T_{\max} \\ & \Theta_2(\mathbf{d}) = V \leq V_{max} \\ & \Theta_3(\mathbf{d}) = R(\mathbf{d}) \leq R_{min}, \end{aligned} \tag{9}$$

where compliance is the product of the displacement and loading vectors in the discretized residual equation, U and P. The system is subject to a temperature constraint, which is applied to the entire domain area, volume constraint, and minimum radius constraint. This optimization can be solved efficiently using standard methods to obtain the topology illustrated in Fig. 7a.

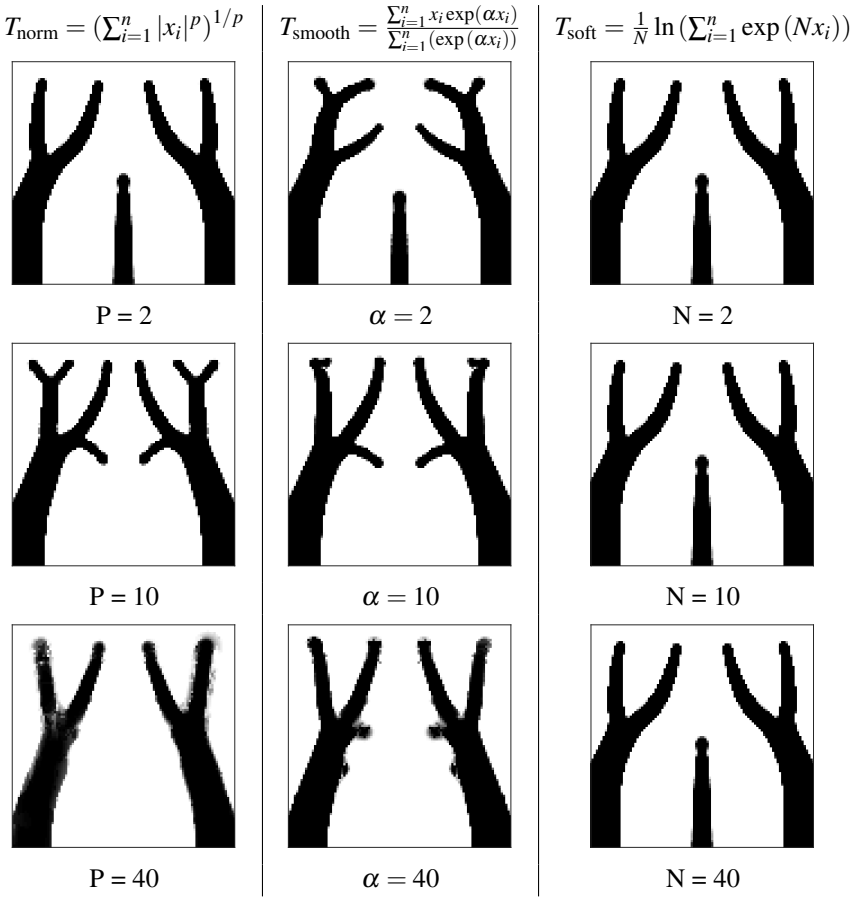

Figure 6: Topological variations based on approximation scaling.

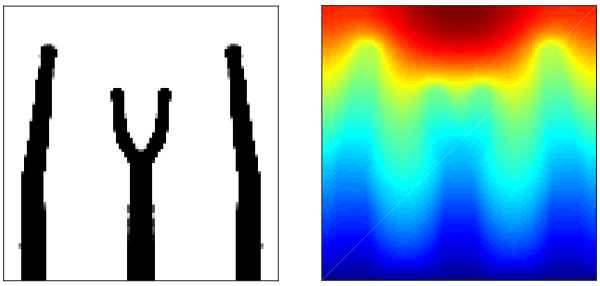

a) Topology b) Temperature

Figure 7: Optimized topology for continuum example.

At the final topology, the approximated temperature varied from the maximum temperature by 10%. This is a reasonable error compared to the large variations observed when using the p-norm. Furthermore, the temperature constraint can be adjusted to account for this difference.

6.2 Discrete Example

This second example considers a design domain more aligned with a power electronics application. The design domain contains four heat sources arranged as shown in Fig. 8. The design domain is 10 cm $\times$ 10 cm, each heating device has an associated 1,000 W volumetric heat generation, and the bottom boundary is fixed at 0. The topology optimization formulation solved here is presented in Eqn. (10):

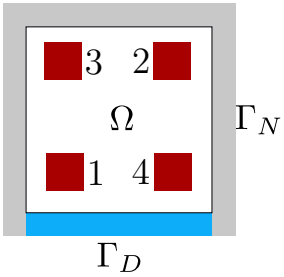

Figure 8: Design domain with four heat sources.

$$\begin{aligned} \min_{\mathbf{d}} \quad & \Theta_0(\mathbf{d}) = \text{ mean } \mathbf{d} \\ s.t. \quad & \Theta_1(\mathbf{d}) = T(\mathbf{d}_{\mathbf{d}3,\mathbf{d}4}) \leq T_{1\max} \\ & \Theta_2(\mathbf{d}) = T(\mathbf{d}_{\mathbf{d}1,\mathbf{d}2}) \leq T_{2\max} \\ & \Theta_3(\mathbf{d}) = R(\mathbf{d}) \leq R_{\min}, \end{aligned} \tag{10}$$

where the objective is to minimize the volume of conductive material subject to two regional temperature constraints. The first temperature constraint is enforced on devices 1 and 2; the second constraint is enforced on devices 3 and 4. These can be thought of as two types of electronic devices with different temperature limitations. The problem is also subject to a minimum volume constraint. The solution to this problem formulation is presented in Fig. 9.

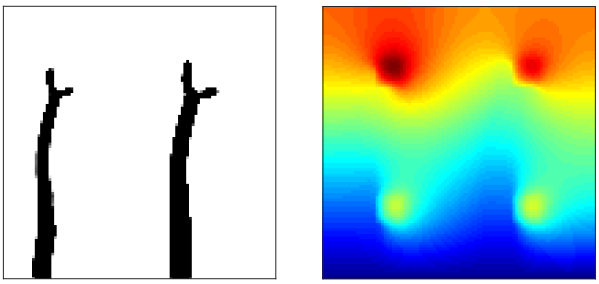

a) Topology b) Temperature

Figure 9: Optimized topology for discrete example.

The optimizer was able to reduce the material required to 9.5% of the domain. Both temperature constraints were satisfied with a 10% margin, the optimizer was slowly removing material as the maximum iteration was reached.

6.3 Temperature Constrained Temperature Minimization

For this next example, consider the same discretely heated design domain as presented in the last example. Here a new topology optimization formulation defined as follows:

$$\begin{aligned} \min_{\mathbf{d}} \quad & \Theta_0(\mathbf{d}) = d_1 \\ s.t. \quad & \Theta_1(\mathbf{d}) = T(\mathbf{d}) \leq d_1 \\ & \Theta_2(\mathbf{d}) = V \leq V_{\max} \\ & \Theta_3(\mathbf{d}) = R(\mathbf{d}) \leq R_{\min}, \end{aligned} \tag{11}$$

where the design vector d is given by:

$$\mathbf{d} = [T_{\max}, x_1, x_2, \ldots x_n]. \tag{12}$$

$T_{\max}$, is the maximum temperature desired, and x_1 through x_n are the elemental material density scalar variables. This type of formulation has been used for optimal control problems where the final time is free. It allows for an increased level of complexity in design where the constraint may vary based on the design. This analogy can be drawn to a printed circuit board design problem, where the temperature constraint may be adjusted by the choice of devices used. Solving this discrete design problem using this formulation results in the topology illustrated in Fig. 10.

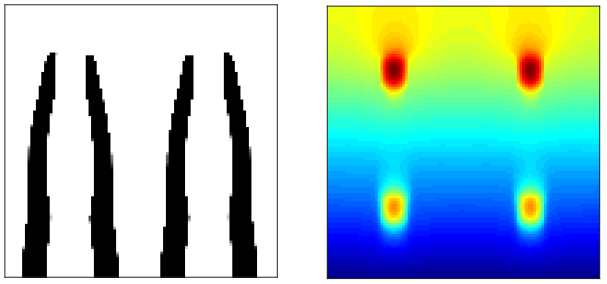

a) Topology b) Temperature

Figure 10: Optimized topology for discrete example.

The optimizer converged to a topology with minimized temperature. For this particular example, it achieves the same solution as a direct temperature minimization. This formulation is solved here to demonstrate that a solution can be achieved with the added constraint variable. Mapping the constraint variable to some design-dependent property is left as a subject for future work.

7. Conlusion

In this work, different approximate maximum functions were investigated for use in temperature-constrained topology optimization. The p-norm, smooth max, and soft max functions were analyzed and tested for topology optimization. It was observed that when scaling the temperature field, the soft maximum function was able to reasonably predict the maximum temperature. Furthermore, when used in optimization, the soft maximum function obtained the same topology independent of scaling parameter value. This is a desirable characteristic for topology optimization, where optimal designs usually vary based on implementation. Using a larger scaling parameter in the soft maximum function, an accurate measure can be obtained for the maximum temperature without causing numerical instabilities in the optimization.

The soft max function was implemented to enforce a global temperature constraint in a compliance minimization problem. It was also used to evaluate regional constraints in two power electronics motivated design problems. These preliminary studies have revealed several promising topics for future investigation. The first of which is to apply the soft maximum function as a temperature constraint in convection dominated problems. Another interesting topic would be to incorporate the design of fan placement and device type using the third formulation presented. Furthermore, measuring the variation in the error in the gradient through optimization iterations would help define the error in the 'optimal' topology. These topics are ongoing research endeavors are left as a subject for future work.

8. Acknowledgments

This material is based upon the work supported by the National Science Foundation Engineering Research Center for Power Optimization of Electro-Thermal Systems (POETS) with cooperative agreement EEC-1449548.

References

Dbouk T (2017) A review about the engineering design of optimal heat transfer systems using topology optimization. Applied Thermal Engineering 112:841–854, DOI 10.1016/j.applthermaleng.2016.10.134, URL http://dx.doi.org/10.1016/j.applthermaleng.2016.10.134

Duysinx P, Sigmund O (1998) New Developments in Handling Stress Constraints in Optimal Material Distribu-

tions. Proceedings of 7th AIAA/USAF/NASA/ISSMO symposium on Multidisciplinary Design Optimization (1):Paper 98–4906, DOI doi:10.2514/6.1998-4906, URL http://hdl.handle.net/2268/17116

Holmberg E, Torstenfelt B, Klarbring A (2013) Stress constrained topology optimization. Structural and Multidisciplinary Optimization 48(1):33–47, DOI 10.1007/s00158-012-0880-7

Le C, Norato J, Bruns T, Ha C, Tortorelli D (2010) Stress-Based Topology Optimization for Continua. Structural and Multidisciplinary Optimization 41:605–620, DOI 10.1007/s00158-009-0440-y

Lohan DJ, Allison JT, Dede EM, Allison JT (2016) Topology Optimization Formulations for Circuit Board Heat Spreader Design. 17th AIAA/ISSMO Multidisciplinary Analysis and Optimization Conference (June):1–8, DOI 10.2514/6.2016-3669, URL http://arc.aiaa.org/doi/10.2514/6.2016-3669

París J, Navarrina F, Colominas I, Casteleiro M (2010) Improvements in the treatment of stress constraints in structural topology optimization problems. Journal of Computational and Applied Mathematics 234(7):2231–2238, DOI 10.1016/j.cam.2009.08.080, URL http://dx.doi.org/10.1016/j.cam.2009.08.080

Zhuang C, Xiong Z (2015) Temperature-Constrained Topology Optimization of Transient Heat Conduction Problems. Numerical Heat Transfer, Part B: Fundamentals 68(4):366–385, DOI 10.1080/10407790.2015.1033306, URL http://www.tandfonline.com/doi/full/10.1080/10407790.2015.1033306